

## SUB-BARRIER FUSION REACTIONS FOR SYNTHESIS OF $^{298}_{114}$

R. A. GHERGHESCU

Horia Hulubei – National Institute for Nuclear Physics and Engineering, P.O. Box MG-6,  
RO-76900, Bucharest, Romania, E-mail: rgherg@ifin.nipne.ro

(Received July 11, 2005)

*Abstract.* Favorable reaction channels are searched for in order to obtain the superheavy element  $^{298}_{114}$ . The interaction energy is supposed to follow the adiabatic hypothesis. As the deformation energy, a very complete binary macroscopic-microscopic energy method is used to perform calculations. Deformed two-center shell model provides the energy level schemes for shell effects. Yukawa-plus-exponential model gives the macroscopic (liquid drop) part of the total energy. The mass tensor is obtained by the Werner-Wheeler irrotational flow hypothesis. Finally the minimization of the multidimensional action integral produces the highest penetrability values. Kr-projectile reactions provide the best pairs, although generally the penetrabilities are very low.

*Key words:* super heavy nuclei, penetrability, fusion interactions, shell corrections.

### 1. INTRODUCTION

The experimental search of the favorized sub-barrier fusion channels for the synthesis of  $^{298}_{114}$  is deterred by the very low cross section and also the low intensity of the incoming ion flux. Cross section decreases with decreasing  $E_{CM}$ , but the present calculations take advantage of obtaining the compound nucleus in the lowest excitation energy, close to its ground state. In this way it might be possible for the superheavy nucleus to be more stable against immediate alpha decay, cluster emission or fission. The main issue this work is supposed to study is the optimum fusion reaction for the lowest possible kinetic energy of the projectile. Choosing a neutron-richer isotope for example, as a projectile, has as a result a substantial change of the cross section [1]. Up to the complete fusion, the system may however be hindered to reach the final compound nucleus by quasi-fission, a situation taken into account in the dinuclear system model [2]. Best isotopic composition has been calculated for cold fusion reactions in [4], by getting the largest product between compound nucleus formation probability and a survival probability. The effect of interchanging neutrons within a given mass asymmetry channel is also studied using the quantum molecular dynamics model [5]. Here isospin influence on the barrier lowering show that neutron richer projectile

enhance the fusion cross section against neutron-rich target. Justification is given by the influence of  $N/Z$  changes in the neck-formed region, hence the study depends on the degree of overlapping as the neck develops. An increase of the neutron number of the target could increase the fusion cross section for light nuclei reactions [6]. For extreme sub-barrier reactions, like it is the case in the present work, fusion paths are obtained as dynamical minimization over the potential energy surfaces. Potential energy surface studies have been also performed within the framework of self-consistent nuclear models like Skyrme-Hartree-Fock and relativistic mean field [7, 8]. It is shown by these authors that shell closures lower the fusion barrier for a given  $(A_p, Z_p)$ ,  $(A_T, Z_T)$  pair, if one suppose cold fusion reactions. The same closure effect is stressed also in a cluster emission type calculation [9]. Rates of fusion obtained from penetrability could be improved by taking into account friction under the barrier [10] or quasifission [3]. Since isobaric reactions for superheavy production are to be studied here, one should mention that, due to the necessity of using neutron-rich partners, possible neutron transfer could take place between nuclei [11].

Potential energy surfaces usually exhibit valleys interpreted as advantageous paths toward complete fusion. Such minimum sequences in deformation energy start at a certain mass asymmetry. In order to obtain the optimal pair  $(A_T, Z_T)$ ,  $(A_p, Z_p)$ , an  $\eta_A = (A_T - A_p)/A$ -path must be browsed in  $Z$ -direction and this is achieved by exhausting all possible isobaric reactions in a  $\eta_A$ -minimum energy channel. The present work studies the sub-barrier fusion reactions leading to the synthesis of  $^{298}114$ . The macroscopic-microscopic method is employed, within the subsequent steps: calculation of the deformation energy using independent intermediary spheroidal deformations of the target and projectile ( $\chi_T = b_T/a_T$ ,  $\chi_P = b_P/a_P$ ), where  $(b_T, a_T)$  and  $(b_P, a_P)$  are spheroid semiaxes, the small semiaxis of the projectile  $b_P$  and the distance between center  $R$  during the overlapping stage as degrees of freedom. This first part of the approach will be applied for the whole range of mass asymmetry  $(A_T, A_p)$  combinations, choosing  $(Z_T, Z_p)$  as the one with the lowest value of total deformation energy for separated target and projectile. The *static* barriers for these pairs are obtained by energy minimization over the multidimensional space of deformation. The second stage of the approach is the repetition of the calculation for all possible isobaric reaction channels inside the promising valleys obtained at the first stage. Final stage is the dynamical calculation. The mass tensor is calculated by means of Werner-Wheeler irrotational flow method. The action integral is then computed for all isobaric reactions with the lowest static barriers. Minimization of the action integral within the 4-dimensional space of deformation will provide the final penetrability value for every cold fusion channel.

Section 2 is a brief presentation of the deformation energy calculation. Section 3 describes the mass tensor components and the dynamical minimization of the action integral. Section 4 is devoted to the results and discussion.

## 2. STATIC BARRIERS

Tip-to-tip configurations for two intersected spheroids are calculated. Binary macroscopic-microscopic method is used to calculate the deformation energy. Single particle energy levels are obtained by the deformed two-center shell model. Details of calculation are given in [12]. In the Schrödinger equation:

$$H\Psi - E\Psi = 0 \quad (1)$$

the total Hamiltonian:

$$H = -\frac{\hbar}{2m_0}\Delta + V(\rho, z) + V_{\Omega_s} + V_{\Omega^2} \quad (2)$$

is deformation dependent. The deformed two-center oscillator potential for target and projectile regions  $v_T$  and  $v_P$  reads:

$$V(\rho, z) = \begin{cases} V_T(\rho, z) = \frac{1}{2}m_0\omega_{\rho_T}^2\rho^2 + \frac{1}{2}m_0\omega_{z_T}^2(z+z_T)^2, & \text{for } v_T \\ V_P(\rho, z) = \frac{1}{2}m_0\omega_{\rho_P}^2\rho^2 + \frac{1}{2}m_0\omega_{z_P}^2(z-z_P)^2, & \text{for } v_P \end{cases} \quad (3)$$

where  $z_T$  and  $z_P$  are the centers of the target and projectile, and equality:

$$V_T(\rho, z) = V_P(\rho, z) \quad (4)$$

defines the border between  $v_T$  and  $v_P$  regions; the relation with the deformations of the two spheroid semiaxes ( $b_i, a_i$ ) is given by the frequency relations:

$$\begin{aligned} m_0\omega_{\rho_i}^2 &= (a_i/b_i)^{2/3} \cdot m_0\omega_{0i}^2 = (a_i/b_i)^{2/3} \cdot 54.5/R_i^2 \\ m_0\omega_{z_i}^2 &= (b_i/a_i)^{4/3} \cdot m_0\omega_{0i}^2 = (b_i/a_i)^{4/3} \cdot 54.5/R_i^2 \end{aligned} \quad (5)$$

where  $R_i = r_0A_i^{1/3}$ , and  $b_i, a_i$  are the spheroid semiaxes.

Since the angular momentum dependent potentials  $V_{\Omega_s}$  and  $V_{\Omega^2}$  depend on  $\nabla V(\rho, z)$ , these terms also follow any changes in the deformation of the partially overlapped fragments. Another deformation-dependent factor is the spin-orbit interaction strength. Its value determines the shell closures for different nuclear mass regions. Since the heavy and light fragment action manifests itself within space regions defined by eq. (4), change of the spin-orbit strength parameter from target to projectile is effectuated within space regions depending on the two semiaxis ratios  $\chi_T = b_T/a_T$  and  $\chi_P = b_P/a_P$ . Usual matrix diagonalization of  $H$  leads to the level scheme of two partially overlapped spheroids for a given distance  $R$  between centers and intermediary (independent)  $\chi_T$  and  $\chi_P$ . The sequence of level schemes are used in the Strutinsky method [13] to compute separately the proton

and neutron shell corrections. This is a very important point of the calculation, especially when one aims to cold fusion of superheavy nuclei. It is well known that these nuclei survive only due to negative shell corrections, their macroscopic barrier being negligible [14]. At certain intermediary deformations ( $\chi_T$  and  $\chi_P$  at given  $R$ ), partially overlapped shells display proton and/or neutron closure and minima are generated in the shell corrections. These minima substantially contribute to the energy valleys.

The macroscopic part is computed with the Yukawa-plus-exponential model. As a peculiarity, the Coulomb  $E_C$  [16] and the nuclear surface term  $E_Y$  [17] are computed as:

$$E_C = \frac{2\pi}{3}(\rho_{eT}^2 F_{C_T} + \rho_{eP}^2 F_{C_P} + 2\rho_{eT}\rho_{eP} F_{C_{TP}}) \quad (6)$$

and

$$E_Y = \frac{1}{4\pi\epsilon_0^2} [c_{sT} F_{EYT} + c_{sP} F_{EYP} + 2(c_{sT}c_{sP})^{1/2} F_{EY_{TP}}] \quad (7)$$

where  $\rho_{ei}$  is the charge density and  $c_{si}$  the surface coefficient.  $F_{C_i}$  and  $F_{EY_i}$  are shape dependent integrals. The last term in paranthesis is the Coulomb and respectively nuclear surface interaction between target and projectile within overlapping [18]. Both  $E_C$  and  $E_Y$  are in that way deformation dependent. The total deformation energy  $E_{def}$  is obtained as:

$$E_{def} = E_{macro} + E_{shell} \quad (8)$$

where:

$$E_{macro} = (E_C - E_C^{(0)}) + (E_Y - E_Y^{(0)}) \quad (9)$$

scaled to the sphere values  $E_C^{(0)}$  and  $E_Y^{(0)}$  and  $E_{shell}$  is the shell correction energy.

### 3. MASS TENSOR AND PENETRABILITY

There are four independent variables describing the configuration of two intersected spheroids: the ratios of the spheroid semiaxes for target  $\chi_T$  and projectile  $\chi_P$ , the small semiaxis of the projectile  $b_P$  (the target semiaxis  $b_T$  results from volume conservation) and the distance between centers  $R$ . From Werner-Wheeler approach [19], the main term reads:

$$B'_{ij} = \int_{z_m}^{z_M} T_{ij}(z; q) dz \quad (10)$$

with:

$$T_{ij} = \rho_s^2(z) \left[ X_i X_j + \frac{1}{8} \rho_s^2(z) \frac{\partial X_i}{\partial z} \frac{\partial X_j}{\partial z} \right] \quad (11)$$

where  $i, j$  are one of the four deformation coordinates and:

$$X_i(z) = \frac{1}{\rho_s^2(z; q)} \frac{\partial}{\partial q_i} \int_z^{z_M} \rho_s^2(z'; q) dz' \quad (12)$$

where  $\rho_s(z)$  describes the surface. A second term in the tensor component is responsible for the correction due to the center of mass motion. It has been calculated here starting from the kinetic energy expression, with discrete velocities of the type  $(\dot{r}_i' - \dot{R}_{CM})$ , and convert the sums into integrals over the whole binary shape configuration. The mass tensor correction components are obtained as:

$$B_{ij}^c = \frac{\sigma_m^2 \pi^2}{M} \left\{ \left[ \int_{z_m}^{z_M} \rho_s^2(z) X_i(z) dz \right] \left[ \int_{z_m}^{z_M} \rho_s^2(z') X_j(z') dz' \right] \right\}$$

where  $M$  is the total mass of the system. Finally the total components of the inertial mass tensor are calculated as:

$$B_{ij} = B_{ij}' - B_{ij}^c \quad (13)$$

In order to perform the further action integrals, it is useful to contract the tensor along one of the coordinates. A first condition in the numerical computation is to impose the projectile volume to decrease by a fixed amount  $\Delta V_p = 0.15V_p$  (arbitrary) at every step value  $R$ , as the projectile enters the target. Second, one complies to the variation law of  $\chi_T$  and  $\chi_P$  such that at the touching point (start of the process) they take initial (separated nuclei) values  $\chi_{T0}$  and  $\chi_{P0}$ . At the end  $\chi_T$  must be equal to the compound nucleus value  $\chi_0$ , while  $\chi_P$  ends at an independent  $\chi_{Pf}$ . There are obviously many functions to describe such a pass. This work proposes a simple linear transition:

$$\begin{aligned} \chi_T &= \chi_{T0} + (\chi_0 - \chi_{T0}) \frac{R - R_f}{R_t - R_f} \frac{100}{k_T} \\ \chi_P &= \chi_{P0} + (\chi_{Pf} - \chi_{P0}) \frac{R - R_f}{R_t - R_f} \frac{100}{k_P} \end{aligned} \quad (14)$$

if  $R < 0.01(R_t - R_f)k_T$  for  $\chi_T$  and  $R < 0.01(R_t - R_f)k_P$  for  $\chi_P$ .  $k_T$  and  $k_P$  are independent number of steps in  $R$  direction with  $k_T, k_P < 100$ , and oblige the

number of steps (or the distance range in  $R$ ) along which the semiaxis ratios change. Also:

$$\chi_{Pf} = \chi_{P0} - \frac{i_p}{10}(\chi_0 - \chi_{P0}) \quad (15)$$

introduces  $i_p$  as another independent parameter, which describes how much the projectile changed its initial semiaxis ratio along the overlapping process. Due to eqs. (14) and (15),  $\chi_T$ ,  $\chi_P$  and  $b_P$  are independent degrees of freedom. Both partners end at the compound nucleus value  $\chi_{Tf} = \chi_0$  and  $\chi_{P0} = \chi_0$ . The lines differ by  $k_T$  (upper plot) and  $k_P$  respectively. In all cases  $b_T$  ends at the same value  $b_0$  of the final compound nucleus semiaxis. For  $b_P$  conditions are more relaxed. The dashed-dotted horizontal line for  $b_P$  represents the case when the projectile does not change its shape and dimensions all along the overlapping process. These considerations lead to the dependence of  $b_P$ ,  $\chi_T$  and  $\chi_P$  on the same parameters:

$$\begin{aligned} \chi_T &= \chi_T(k_T, k_P, i_p; R) \\ b_P &= b_P(k_T, k_P, i_p; R) \\ \chi_P &= \chi_P(k_T, k_P, i_p; R) \end{aligned} \quad (16)$$

The number of steps  $k_T$ ,  $k_P$  and  $i_p$  are varied numerically within such range that  $b_0 > b_P \geq b_{P0}$  and  $\chi_T \in (\chi_0, \chi_{T0})$  and  $\chi_P \in (\chi_{Pf}, \chi_{P0})$ . The above functions allow to obtain numerically the derivatives to  $R$ . Final contracted total mass inertia becomes:

$$\begin{aligned} B(R) &= B_{b_P b_P} \left( \frac{db_P}{dR} \right)^2 + 2B_{b_P \chi_T} \frac{db_P}{dR} \frac{d\chi_T}{dR} + 2B_{b_P \chi_P} \frac{db_P}{dR} \frac{d\chi_P}{dR} + \\ &+ 2B_{b_P R} \frac{db_P}{dR} + B_{\chi_T \chi_T} \left( \frac{d\chi_T}{dR} \right)^2 + 2B_{\chi_T \chi_P} \frac{d\chi_T}{dR} \frac{d\chi_P}{dR} + \\ &+ 2B_{\chi_T R} \frac{d\chi_T}{dR} + B_{\chi_P \chi_P} \left( \frac{d\chi_P}{dR} \right)^2 + 2B_{\chi_P R} \frac{d\chi_P}{dR} + B_{RR} \end{aligned} \quad (17)$$

It is important to emphasize that the above laws of variation restrict by no means the system to follow a certain path. The final fusion path is obtained as the result of minimization over *all* the possible values (hence all range of  $\kappa_T$ ,  $\kappa_P$ ,  $i_p$ ) in *any* direction at a fixed  $R$ . Thus, when the action integral is minimized, the configuration follows an energy valley which is not necessary along one of the variation laws indicated above. The system simply can switch from one set of  $(\kappa_T, \kappa_P, i_p)$  to another set  $(\kappa'_T, \kappa'_P, i'_p)$  at successive  $R$ -steps.

Penetrability  $P$  for a given fusion path is calculated as usual:

$$P = \exp(-K_{ov}) \quad (18)$$

where  $K_{ov}$  is the overlapping action integral. The barriers are supposed to be tunneled at the level of the final compound nucleus ground state. This is the minimum value of the kinetic energy in this work where sub-barrier fusion reactions are intended to take place at the lowest energy.  $K_{ov}$  is calculated numerically as:

$$K_{ov}(b_P, \kappa_T, \kappa_P; R) = \frac{2}{\hbar} \int_{(fus)} [2B(R)_{b_P, \kappa_T, \kappa_P} E_{def}(R)_{b_P, \kappa_T, \kappa_P}]^{1/2} dR \quad (19)$$

Since  $K_{ov}$  is calculated for every set  $(b_P, \kappa_T, \kappa_P)$  at every point  $R$ , the penetrability presents itself as a multidimensional lot. The final value of  $P$  for every channel reaction is the result of action integral  $K_{ov}$  minimization over the whole range of  $(b_P, \kappa_T, \kappa_P, R)$ .

#### 4. RESULTS AND DISCUSSION

The deformation energy is computed for every possible  $(A_T, A_P)$  fusion channel leading to the same compound nucleus. Calculations are performed for  $^{298}114$ . Mass asymmetries start from  $\eta_A = 0$  with symmetric reaction  $^{148}\text{Ba} + ^{150}\text{Ce}$  up to  $\eta_A \approx 0.84$  corresponding to  $^{18}\text{O} + ^{280}\text{No}$ .

The numerical results are presented in Fig. 1 as a potential energy surface. Total deformation energy is drawn as a function of the distance between centers  $R$  and mass asymmetry  $\eta_A$ . There are two energy valleys: a symmetrical one around  $\eta_A = 0$  and a second valley at about  $\eta_a = 0.28$ . The best reaction pairs are marked on the figure. The entrance points in the barriers are more deeper into the overlapping configuration than for the neighbouring pairs.

The action integral has been minimized for  $(A_T, A_P)$  between (168, 130) and (190, 108), browsing the energy valley around  $\eta_A \approx 0.3$ . Isobaric reactions with all obtainable (stable) partners are subjected to calculation in order to reveal first the isospin influence within the same  $\eta_A$  and then to obtain the maximum penetrability.

The resulted penetrabilities are presented in Table 1, for  $^{298}114$ . The best penetrability value seems to encourage  $^{146}\text{Xe} + ^{152}\text{Nd}$  to be used as a sub-barrier fusion reaction to be used in the synthesis of  $^{298}114$ .

As a final remark, we state that the extreme sub-barrier fusion as an alternative to high energy synthesis reaction has certainly the disadvantage of having a very low probability, hence a low cross section. However, the final compound nucleus could be synthesized in a more stable state (no excitation), thus it probably lives longer. Within the presented adiabatic approach, the favorable reaction mentioned above does have a rather low penetrability value for cold

fusion, but could be used for such experiments to synthesize  $^{298}114$ . None of the reactions took advantage of proton and/or neutron magicity.

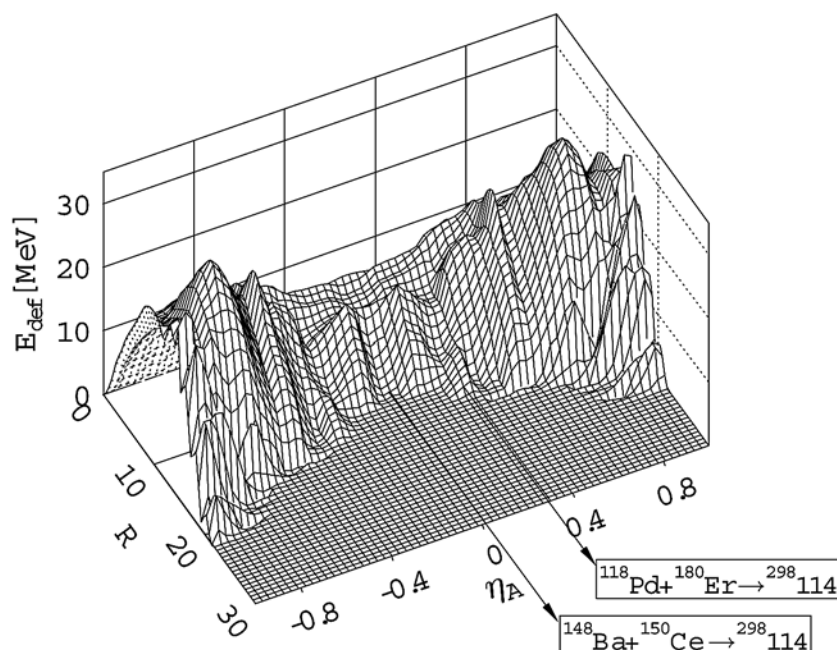


Fig. 1 – Potential energy surface calculated for  $^{298}114$  synthesis reaction channels as a function of the distance between centers and mass asymmetry.

Table 1

The dynamic barriers  $E_b$  and logarithms of penetrabilities  $\log_{10}P$  for the energy valley in synthesis of  $^{298}114$

Reaction	$E_b$ [MeV]	$\log_{10}P$
$^{148}\text{Xe} + ^{150}\text{Nd}$	9.72	-25.299
$^{148}\text{Ba} + ^{150}\text{Ce}$	9.60	-25.111
$^{148}\text{Ce} + ^{150}\text{Ba}$	9.74	-26.044
$^{146}\text{Xe} + ^{152}\text{Nd}$	9.76	-24.855
$^{146}\text{Ba} + ^{152}\text{Ce}$	9.75	-25.832
$^{144}\text{Xe} + ^{154}\text{Nd}$	9.69	-25.816
$^{144}\text{Ba} + ^{154}\text{Ce}$	10.24	-27.858
$^{142}\text{Te} + ^{156}\text{Sm}$	9.69	-26.029
$^{142}\text{Xe} + ^{156}\text{Nd}$	9.71	-27.963
$^{140}\text{Te} + ^{158}\text{Sm}$	9.80	-27.327
$^{140}\text{Xe} + ^{158}\text{Nd}$	10.46	-29.512
$^{138}\text{Sn} + ^{160}\text{Gd}$	12.09	-29.405
$^{138}\text{Te} + ^{160}\text{Sm}$	12.70	-30.563

## 5. CONCLUSIONS

When nuclei approach to each other with a kinetic energy equal to the  $Q$ -value of the reaction, chances are to obtain a compound nucleus very close to its ground state. Since no excitation triggers a decay process, the final system could be more stable and live longer. The space of deformation that has been used to obtain the results of this work includes a complete number of parameters to describe head-on collisions of spheroidally deformed partners. Different semiaxis ratios of the target and projectile during the overlapping region and variable projectile semiaxis  $b_p$  insure new degrees of freedom in the microscopical shell level calculation, and finally in obtaining the total deformation energy and mass tensor. The present approach used a binary model to study the dynamics of possible sub-barrier fusion reactions towards the synthesis of two superheavy isotopes. Xe-accompanied reaction could be used in a trial experiment, to obtain  $^{298}114$  in a close to ground state energy, by using a kinetic energy equal to the  $Q$ -value.

## REFERENCES

1. S. Hofmann and G. Münzenberg, *Rev. Mod. Phys.*, **72**, 733 (2000).
2. N. V. Antonenko, E. A. Cherepanov, A. K. Nasirov, V. P. Permjakov and V. V. Volkov, *Phys. Rev.*, **C51**, 2635 (1995).
3. G. G. Adamian, N. V. Antonenko and W. Scheid, *Phys. Rev.*, **C68**, 034601 (2003).
4. G. G. Adamian, N. V. Antonenko and W. Scheid, *Phys. Rev.*, **C69**, 011601(R) (2004).
5. Ning Wang, Xizhen Wu and Zhuxia Li, *Phys. Rev.*, **C67**, 024604 (2003).
6. K. Satou, H. Ikezoe, S. Mitsuoka, K. Nishio and S. C. Jeong, *Phys. Rev.*, **C65**, 054602 (2002).
7. M. Bender, K. Rutz, P-G. Reinhard, J. A. Maruhn and W. Greiner, *Phys. Rev.*, **C58**, 2126 (1998).
8. J. F. Berger *et al.*, *Nucl. Phys.*, **A685**, 1 (2001).
9. M. Goncalves and S. B. Duarte, *Phys. Rev.*, **C48**, 2409 (1993).
10. B. G. Giraud, S. Karataglidis, K. Amos and B. A. Robson, *Phys. Rev.*, **C69**, 064613 (2004).
11. V. I. Zagrebaev, *Phys. Rev.*, **C67**, 061601(R) (2003).
12. R. A. Gherghescu, *Phys. Rev.*, **C67**, 014309 (2003).
13. V. Strutinsky, *Nucl. Phys.*, **A95**, 420 (1967).
14. A. Sobiczewski, *Phys. Part. Nucl.*, **25**, 295 (1994).
15. Z. Patyk and A. Sobiczewski, *Phys. Lett.*, **B256**, 307 (1991).
16. K. T. Davies and A. J. Sierk, *J. Comp. Phys.*, **18**, 311 (1975).
17. H. J. Krappe, J. R. Nix and A. J. Sierk, *Phys. Rev.*, **C20**, 992 (1979).
18. D. N. Poenaru, M. Ivascu and D. Mazilu, *Comp. Phys. Comm.*, **19**, 205 (1980).
19. K. T. Davies, A. J. Sierk and J. R. Nix, *Phys. Rev.*, **C13**, 2385 (1976).
20. R. A. Gherghescu, J. Skalski, Z. Patyk and A. Sobiczewski, *Nucl. Phys.*, **A651**, 237 (1999).
21. P. Möller, J. R. Nix and K-L. Kratz, *At. Data Nucl. Data Tables*, **66**, 131 (1997).
22. H. Esbensen, *Phys. Rev.*, **C68**, 034604 (2003).